

MODELING THE SEAT BELT TO SHOULDER-COMPLEX INTERACTION IN FAR-SIDE CRASHES

Clay A. Douglas

Brian N. Fildes

Monash University Accident Research Centre
Australia

Tom J. Gibson

Human Impact Engineering
Australia

Ola Boström

Autoliv Research
Sweden

Frank A. Pintar

Medical College of Wisconsin and VA Medical Center
United States of America
Paper Number 07-0296

ABSTRACT

Regulations and interventions to protect far-side occupants in crashes do not currently exist, despite these occupants accounting for 43% of the AIS3+ injured persons and 30% of the overall Harm in side impact crashes. Furthermore, no suitable ATDs or mathematical models have been developed to investigate far-side occupant dynamics. The aim of this study was to investigate seat belt to shoulder-complex interaction during the first phase of a far-side impact for incorporation into a multibody occupant model.

The model adaptations were derived based on quasi-static belt slip tests using two volunteers, a standard Hybrid III ATD and a Hybrid III Spring-Spine ATD. The model development was validated for this first phase of impact by comparison with shoulder belt force-time histories and head lateral displacements from lateral far-side sled tests using PMHS and a WorldSID ATD.

The newly adapted model correctly predicted seat belt to shoulder complex interaction in all of the quasi-static belt slip tests, compared to 50% and 67% for Hybrid III and Hybrid III Spring-Spine respectively. Furthermore, the model was able to predict the increasing likelihood of the seat belt engaging the shoulder when the D-ring moved rearward and pretension increased. For the validation tests, the magnitude and phasing of the shoulder-belt force-time and head displacement-time histories were generally within 10% of the PMHS results. In addition, the model was capable of predicting the location of occupant to seat belt interaction observed in the PMHS tests.

INTRODUCTION

Side impacts represent the second most common type of passenger vehicle crash to cause serious injury or death to the occupant behind frontal collisions (Fildes et al., 1991; Otte, 1984). Research into side impact is becoming more critical as it is projected that the number of elderly road users will increase. Elderly road users have an increased likelihood of being involved and seriously injured in a side impact crash compared to other age groups (Chipman, 2004).

In addition, while research attention and government regulations have focused on protecting nearside (or struck side) occupants of the vehicle, little attention has been paid to protecting far-side (or non-struck side) occupants. Research by Gabler et al. (2005a) using NASS/CDS and FARS data from 1997-2002 indicated that far-side occupants account for 43% of the seriously injured persons and 30% of the Harm in US side impact crashes. Furthermore, using MUARC in-depth data (MIDS) from 1993-2002, Gabler et al. (2005b) observed that far-side occupants accounted for 20% of the seriously injured persons and 24% of the Harm in Australian side impact crashes.

The primary form of restraint for a far-side occupant is the outboard mounted three-point seat belt. However, it has been recognized that this design does not provide adequate restraint for this crash configuration. Specifically, by preventing thorax and head excursion towards the struck side of the vehicle. This was most recently highlighted by Gabler et al., (2005a) where head and thorax injuries accounted for over half of the serious injuries sustained in these crashes. Added to that, the seat belt has been recorded as the source of injury in around 86% of

AIS2+ abdominal injuries sustained in far-side crashes (Gabler et al. 2005a).

In an earlier study, Mackay et al., (1993) conducted an analysis of 193 cases of restrained occupants in far-side crashes. It was observed that of those occupants with AIS ≤ 2 head injuries, 35% came out of the shoulder section of the seat belt. The authors suggested that "...as well as the direction of the impact, a number of other factors have a bearing on this event – the position of the upper anchorage, the size of the occupant, the seat position, the adjustment of the upper anchorage, and the looseness of the seat belt". Mackay concluded by stating that these problems may be alleviated through experimental work looking at improving seat belt geometry and pretensioning.

It had long been recognized that the seat belt was not ideal in all crash configurations. Knowing this, early laboratory studies by Adomeit et al., (1977) and Horsch (1980) examined the effect of impact angle on the restraint provided by the seat belt using anthropomorphic test devices (ATDs). Both Adomeit et al., (1977) and Horsch (1980) observed that for far-side impacts up to approximately to 40 degrees, the shoulder belt remained in the clavicular area and did not slip off the shoulder. At angles greater than this the thorax tended to slip out of the shoulder portion of the seat belt, leading to an increase in thoracic and head excursion. Horsch did however note that even at angles of around 60 degrees, significant energy was removed from the thorax by the seat belt before slippage.

In an attempt to reduce this lateral excursion, Horsch et al., (1979) and Kallieris & Schmitt (1990) used Post Mortem Human Subjects (PMHS) to investigate the effect of inboard belts. However, such designs were observed to induce neck injuries. One of the primary concerns with the use of an inboard belt is this neck loading, which can place the neck's vascular system and spinal column at risk of trauma (Sinson et al., 2003).

More recent attempts have been made to reduce occupant excursion towards the vehicle's struck side in a far-side crash (Stolinski et al., 1999; Boström & Haland, 2003; Pintar et al., 2006; Rouhana et al. 2006). Stolinski et al., (1999) investigated the effect of firing pretensioners on reducing lateral excursion using Hybrid III and SID ATDs. Boström and Haland (2003) investigated inboard airbags and a 3+2 seat belt design using a modified BioSID ATD; Pintar et al. (2006) investigated thorax and shoulder supports in addition to inboard belts using a WorldSID ATD;

and Rouhana et al. (2006) investigated the use of a four-point seat belt using PMHS, BioSID and SIDII ATDs. Each study suggested methods of reducing head and thorax excursion, however, more research is required to ensure that these designs do not induce additional injuries, primarily to the thorax and neck.

Despite these attempts to design better restraints, therein lies a problem, no computer model or ATD is designed specifically for far-side impacts. WorldSID has been suggested to be the best of the available ATDs (Fildes et al., 2002), however, thorough validation is yet to be seen. A major limitation ATDs have is the ability to mimic the seat belt to shoulder complex interaction. This has come primarily from the fact that ATDs are designed to work within a narrow crash configuration band. In frontal crash tests, Hybrid III ATDs only have a single measurement device in the chest to measure the effect of shoulder belt load. However, up to half the belt load gets distributed through the shoulder where no measurement device exists (Kent et al., 2003). In side impacts, ATDs are to a large extent not validated using shoulder belts. As a result, the shoulder region of both frontal and side impact dummies is not ideal.

Tornvall et al., (2005) investigated this very aspect, more specifically looking at the performance of the shoulder complex of THOR in oblique impacts (both near and far-side). Despite a lack of sufficient PMHS tests in far-side configurations, Tornvall's results indicate a weakness in the kinematic shoulder response of the three ATDs, possibly related to limitations in shoulder range-of-motion and the lack of human-like shoulder complex design (Tornvall et al., 2005).

This investigation forms part of a larger study aimed at improving far-side occupant protection (Fildes et al., 2005). A subtask of this larger study involves developing a far-side occupant model. Due to the critical role of seat belt to shoulder-complex interaction in governing upper body kinematics in a far-side crash, it was deemed necessary to explore further.

OBJECTIVE

The aim of this study was to investigate seat belt to shoulder-complex interaction during the first phase of a far-side impact and incorporate this knowledge into a multibody occupant model.

METHODS

This study is separated into four components: quasi-static far-side tests categorizing the seat belt to shoulder-complex interaction; developing a model capable of mimicking this interaction; high-speed lateral far-side sled tests; and validating the model against these sled tests.

1g Quasi-Static Far-Side Tests

The aim of the quasi-static belt slip tests was to characterize the seat belt to shoulder-complex interaction in a far-side impact. Two factors identified by Mackay et al., (1993) – seat belt geometry and pretension, were investigated regarding their role in providing lateral restraint to the subject.

To achieve these aims, a test rig consisting of a rotating seat with appropriate safety measures was designed (Figure 1). It rotated the subject in the frontal plane, about an axis running horizontal to the ground through their thorax. When rotated 90 degrees, the subject experienced a 1g lateral force.



Figure 1. Rotating quasi-static test rig

The test subject was seated normally with the belt in the drivers position in a Volvo V70 seat. The seat back was positioned to the angle used in seat rating tests, the tilt and other chair settings being set to the mid-positions and were kept there throughout testing.

The seat X-position (fore/aft) was instrumented such that 5 positions: 0, 60, 120, 180, and 240 could be determined. These positions (measured in millimeters from most-rearward) represented 0%, 25%, 50%, 75%, and 100% forward. Similarly, this represents moving the D-ring fore/aft (0 being the most forward D-ring, 240 being the most rear D-ring).

In addition to belt geometry, three belt pretensions were tested. Due to the difficulty in getting reproducible tensions, ranges were used instead of specific tensions. These were 0N, 100-150N, and 200-250N. The tension was produced prior to the test manually (not through actual pretensioner devices) and measured through a standard belt tension measurement system (Figure 2) and monitored from a continuous online display.



Figure 2. Seat belt tension measurement device and anchorage point

Three different subjects were put through the entire matrix of tests: A standard Hybrid III 50th Percentile Male ATD; A Hybrid III 50th Percentile Male with a Spring-Spine (as seen in Boström et al., 2005); and a male human volunteer of average height and weight. For the volunteer test, muscle tension was neglected as the subject was completely relaxed, with little or no muscle activity.

A second volunteer was exposed only to the X = 120, 0N pretension configuration to highlight the difference body size has on the resulting restraint. The second volunteer was more muscular and broad shouldered than the first volunteer. Volunteer 1's shoulder breadth was approximately 480mm, whereas the second volunteer's was 560mm.

The only measured outcome from these tests was whether the seat belt slipped off the shoulder or not, leading the results to be binary (i.e. yes or no). Five tests were conducted with each subject at the same configuration. As such, a percentage of times the belt slipped off the shoulder for each configuration could be determined. For instance, if the belt slipped off the shoulder in 5 out of 5 cases at a set configuration, the result would be 100%. If the belt only slipped twice, the result would be 40% and so on.

Modeling the 1g Quasi-Static Far-Side Tests

The test set-up geometry (as described in the previous section) was modeled in MADYMO 6.2.2 using the pre-processor Easi-Crash-MAD v5. A geometrically similar seat and seat belt was modeled using facet surfaces and finite elements respectively. Each was given realistic stiffness characteristics.



Figure 3. Human model in simulated 1g test

The human model used for these simulations was the TNO Human Facet Model. This model was recently validated against ISO TR9790 requirements for lateral impact by de Lange et al., (2005). The same study also demonstrated that the human facet model showed potential in frontal and oblique impacts (de Lange et al., 2005). The human facet model was identified to be the most suitable MADYMO model for far-side impacts (Digges et al., 2005).

As previously mentioned, modeling the seat belt to shoulder-complex interaction is a critical requirement of a far-side occupant model. The standard TNO Human Facet Model is not capable of replicating the contour variation of the shoulder-complex's boney structures, specifically the junction of the clavicle, scapula and humerus.

To address this issue, rigid ellipsoids were inserted into the region of the shoulder (Figure 4). The shoulder was represented by a sphere (degree 2 ellipsoid) of radius 0.053m. These dimensions coincide with those defined for a 50th percentile male in Tilley et al., (2002). The shoulder breadth of the human model was approximately 460mm.

Two additional ellipsoids were placed in the upper arm adjoining the shoulder ellipsoid to ensure the belt did not deeply penetrate the arm and get caught when the belt slipped off the shoulder. Each was modeled as a sphere of 0.045m radius, which coincides with the same arm thickness defined for arm ellipsoids in earlier versions of the TNO Human Facet Model.

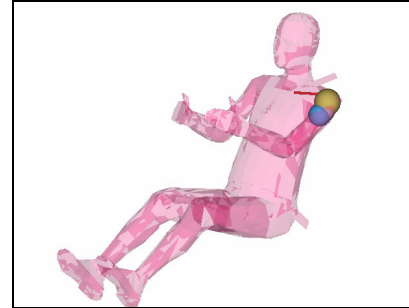


Figure 4. Rigid ellipsoids used to approximate the shoulder on the human model

A MB.FE Kinematic contact was then defined between the seat belt, clavicle and shoulder, so that the belt would not penetrate this region - ensuring the contour of the region (despite being approximated) is maintained. Due to the choice of contact type, a static friction coefficient for the belt and skin interaction could only be defined, rather than a specific velocity dependant function. As such, an approximated friction coefficient of 0.3 was used.

To start the simulation, the human model was firstly sat in the seat under gravity and allowed to come to equilibrium. Belts were then routed across the model such that anchor locations matched those used in the tests. For cases with pretension, simulated loads represented the middle of the ranges defined in the physical tests. To achieve this preload, linear belt segments were attached vertically from the D-ring with 125N and 225N loads added to the ends. This initiated initial penetrations in the model, which provided the preload prior to initiating the lateral 1g pulse.

Once the model was at equilibrium and the belts were in the correct position, a 1g lateral pulse was inserted to the model. This pulse was not a step input, rather a ramp, due to the rotating of the buck in the physical tests. Concurrently, the 1g used for pre-simulation (vertical direction) was ramped down. Each simulation lasted 1 second.

The measured outputs from the model included whether the belt slipped or not, and T1 lateral displacement – to quantify the effect of D-ring position and pretension on excursion.

Far-Side Lateral Sled Tests

Data from lateral far-side sled tests were utilized as means of model validation in this first phase of impact. Tests were conducted at 30km/h using a unique far-side impact buck which included, as a

standard configuration, a center console and outboard three-point belt system (Pintar et al. 2006).

For this study, two configurations of seat belt geometry and pretension were investigated with PMHS and a WorldSID ATD (Table 1). As a realistic worst case scenario, the Forward D-ring was located 120mm above and 30mm rear of the shoulder. The Middle D-ring was located 120mm above and 90mm rear of the shoulder. PMHS tests were conducted using the same procedures as described for the WorldSID tests (Pintar et al., 2006).

Table 1.
Sled Test Matrix

D-Ring Position	Pretension	Test Subject
Middle	100N	PMHS 1, WorldSID
Forward	0N	PMHS 2, WorldSID

For the PMHS tests, 2 unembalmed human cadavers were procured, medical records assessed and tested for Hepatitis A, B, C and HIV. Pretest x-rays and anthropomorphic data were obtained using established procedures (Pintar et al., 1997) (Table 2). PMHS were cleaned then dressed in a tight-fitting leotard with a head/face mask to ensure anonymity.

Table 2.
PMHS Sex and Anthropometry

PMHS	Sex (M/F)	Height (m)	Weight (kg)
1	M	1.73	67
2	F	1.60	70

To quantify occupant-to-seat belt interaction, seat belt force transducers mounted between the shoulder and D-ring measured shoulder belt load. To quantify lateral excursion, retro-reflective targets placed on the head, in addition to reference targets fixed to the sled and buck tracked three-dimensional, 1000 f/s motion (Pintar et al., 2006).

Modeling the Far-Side Sled Tests

The test set-up geometry (as described in Pintar et al. 2006) was modeled in MADYMO 6.2.2 using the pre-processor Easi-Crash-MAD v5 (Figure 5). The sled pulses used from the physical tests were directly inserted into the model. The same human model (including shoulder modifications) was used and executed in the quasi-static tests.

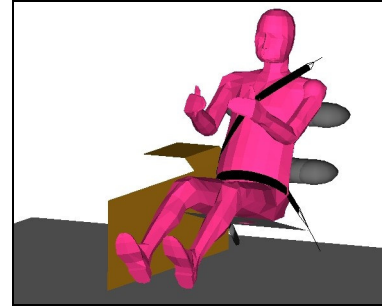


Figure 5. Human model in simulated far-side buck

Seat belts were modeled using finite elements and the center console was modeled using facet surfaces. Force-deflection characteristics for the center console and belts were defined in Pintar et al. (2006).

Within the model, contact between the human model and the center console was defined as a FE.FE (facet-to-facet) COMBINED contact. To achieve this, a stress-strain relationship was required for the paper honeycomb mounted to the console. This was approximated, since the honeycomb's rating was 15psi and 30psi respectively. This approximation can be seen in Figure 6.

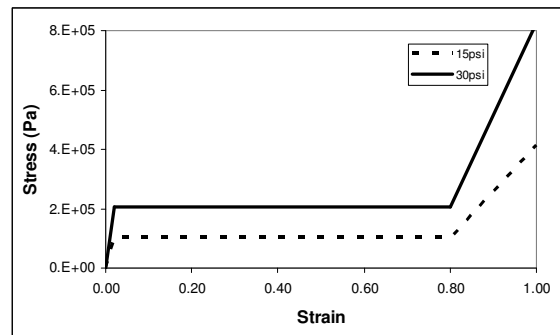


Figure 6. Approximated stress-strain relationship for paper honeycomb

Each simulation was executed for 240ms. The shoulder belt forces and head c.g lateral displacements were obtained from the relevant MADYMO output files.

RESULTS

1g Quasi-Static Far-Side Tests

Results from the physical tests and the simulations can be seen in Table 3. Only results from the four rearmost positions are shown as the most-forward D-ring (X=0) yielded the same result as X=60 Volunteer 1.

Table 3.
1g quasi-static test results. Numbers represent the proportion of time slip occurred at that configuration. Shading represents cases which match volunteer response

VOLUNTEER			
X pos (mm)	0N	100-150N	200-250N
60	100	100	100
120	100	100	20
180	100	0	0
240	100	0	0

HUMAN MODEL			
X pos (mm)	0N	125N	225N
60	100	100	100
120	100	100	0
180	100	0	0
240	100	0	0

HYBRID III SPRING-SPINE			
X pos (mm)	0N	100-150N	200-250N
60	100	60	0
120	100	0	0
180	0	0	0
240	0	0	0

HYBRID III			
X pos (mm)	0N	100-150N	200-250N
60	60	0	0
120	0	0	0
180	0	0	0
240	0	0	0

Results from the volunteer tests indicate that a trend exists between moving the D-ring rearward, increasing pretension, and thus, an increased likelihood of the belt engaging the shoulder. A visual example of cases where belt slip occurred and where the shoulder was engaged can be seen in Figure 7.



Figure 7. Volunteer in cases indicative of belt slip (left) and shoulder engagement (right)

As previously mentioned, the second volunteer was only tested in the X=120, 0N pretension case. For this configuration, the seat belt effectively restrained the larger occupant. Despite this only being a single configuration, it suggests that human anthropometry plays a major role in whether the belt restrains the human or not. It also suggests that more broad or muscular occupants may be better restrained by an outboard three-point belt in a far-side impact.

Results also highlight that the standard Hybrid III and the Hybrid III Spring-Spine ATDs are much more sensitive to changes in belt geometry and pretension than the human volunteer. Moreover, the standard 50th percentile Hybrid III and Hybrid III Spring-Spine only predicted the same binary outcome of slip or engagement in approximately 50% and 67% of the configurations when compared to the mid-sized volunteer. A visual example for the Hybrid III Spring-Spine in cases of belt slip and restraint can be seen in Figure 8.

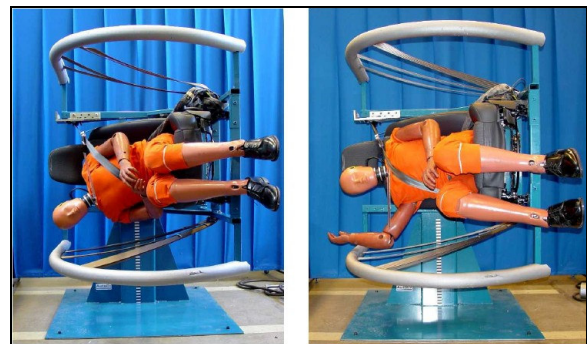


Figure 8. Hybrid III Spring-Spine in cases of belt slip (left) and shoulder engagement (right)

The difference between the way in which the volunteer and the ATDs interacted with the belt was noticeable. Specifically, the belt engaged the ATDs thorax instead of the shoulder complex. Of the two ATDs tested, the Hybrid III Spring-Spine ATD was more biofidelic in how belt slip occurred compared to the standard Hybrid III. However, the Hybrid III Spring-Spine was still more sensitive to D-ring position and pretension than the volunteer. This was related to the solid features of the thorax engaging the belt even when the belt slipped over the shoulder.

Conversely, the human model correctly predicted all of the binary outcomes from the mid-sized volunteer tests, in addition to the trend observed between D-ring position, pretension and belt slip. A visual example of cases where belt slip occurred and where the shoulder was engaged can be seen in Figure 9.

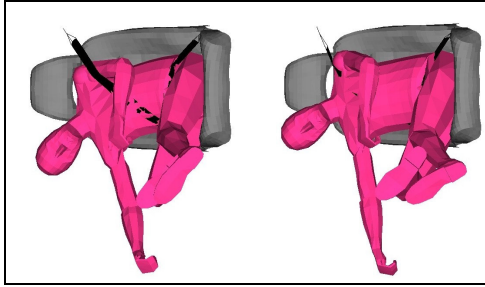


Figure 9. Human model in cases indicative of belt slip (left) and shoulder engagement (right)

Despite the match in binary results, the human model's upper body lateral motion appears stiffer than the volunteer. This is not surprising since this model (like the ATDs) is designed to perform at higher severity impacts than 1g.

In addition to the binary outcomes from the quasi-static tests, T1 lateral displacements were also plotted (Figures 10 and 11). This was done to quantify the effect different D-ring positions and pretensions had on the model's lateral displacement.

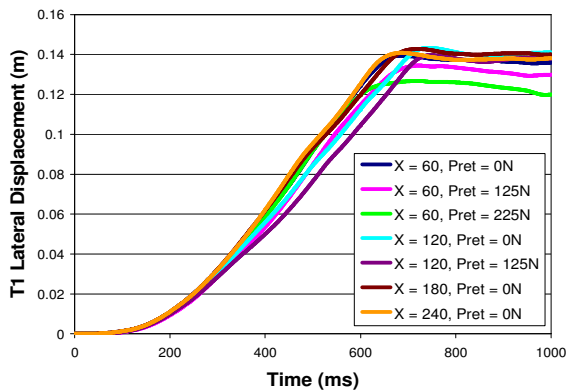


Figure 10. T1 lateral displacement vs. time for cases with belt slip

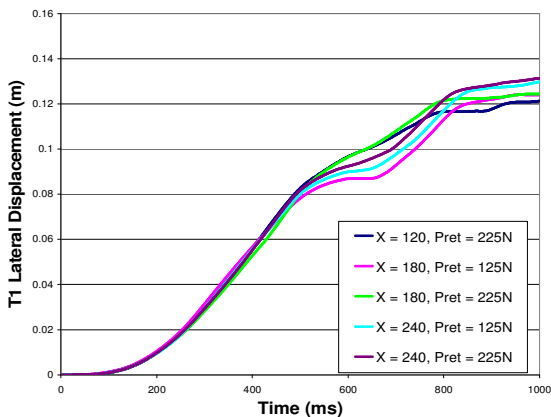


Figure 11. T1 lateral displacement vs. time for cases with belt engaging the shoulder

These results indicate that the crucial factor influencing the magnitude of lateral displacement is whether the belt slips over the shoulder or not. For cases where the belt slips over the shoulder, T1 displacements are all very similar (average displacement = 138mm). When the belt engages the shoulder there is only minor differences between D-ring positions (average displacement = 126mm). What is interesting to note is that this equates to only an average 9% reduction in lateral displacement. It should be noted however that the maximum displacements for cases with slip occurred approximately 200ms earlier than those with engagement.

Far-Side Lateral Sled Tests

For the Middle D-ring configuration, all test subjects indicated that the seat belt engaged the shoulder complex. This can be derived from the shoulder belt force-time histories seen in Figure 12, with an image of the human model response seen in Figure 13.

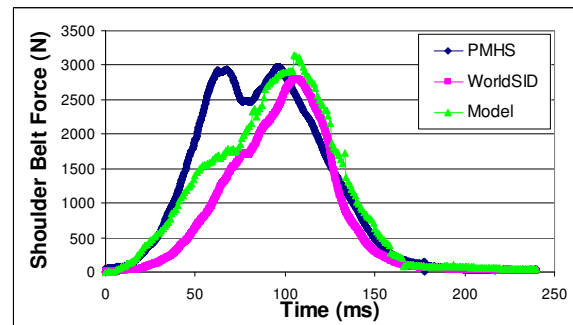


Figure 12. Shoulder belt force – Middle D-Ring, 100N Pretension

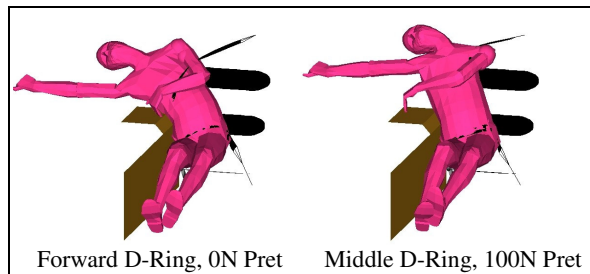


Figure 13. Human model simulated belt interaction in sled tests (175ms)

In the force-time curve, the belt to shoulder-complex interaction is represented by the large peak response at around 100ms. Both the WorldSID and the human Model predicted the magnitude and timing of this event within 10% of the results from the PMHS test. One difference is the initial peak observed in the

response of the PMHS test. This was attributed to thoracic loading prior to slipping across the thorax (drop in response) and then engaging the shoulder. Neither the WorldSID nor human model observed this response to the same magnitude.

For the forward D-ring configuration, all test subjects (PMHS, WorldSID and human model) slipped out of the shoulder portion of the seat belt. In all cases, the belt provided restraint via loading the thorax in the early phases of impact. The belt subsequently slipped past the shoulder and got caught on the upper arm near the elbow. Despite those similarities, the shoulder belt force-time histories are quite different for all three subjects (Figure 14).

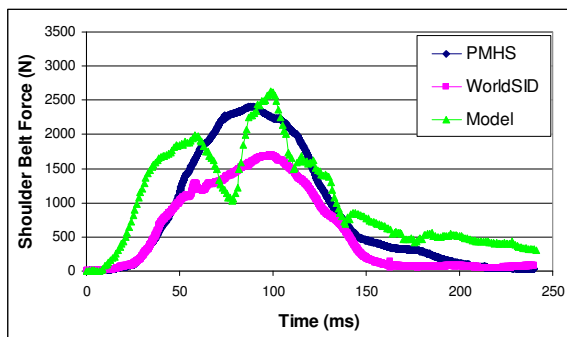


Figure 14. Shoulder belt force – Forward D-Ring, 0N Pretension

The shape and phasing of WorldSID and PMHS traces are similar, however the magnitude of the PMHS belt force is 40% higher than WorldSID. Conversely, the human model made a closer match of the belt force magnitude, however the trace shows a profound double peak. The first peak related to the thorax loading the belt, with the second peak for contact with the upper arm. This suggests that the thorax of the PMHS and WorldSID took nearly all the belt load. Whereas in the model, belt load dropped whilst the belt slipped over the shoulder.

To quantify excursion, head lateral displacements were plotted versus time for both test configurations (Figures 15 and 16).

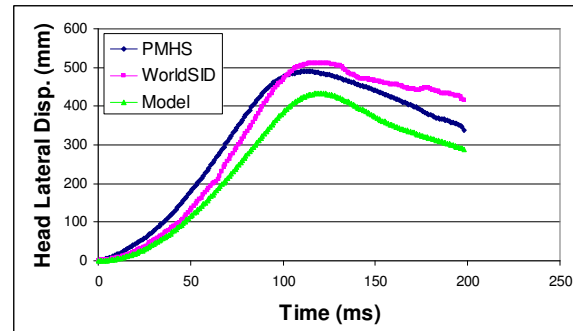


Figure 15. Head lateral displacement – Middle D-ring, 100N Pretension

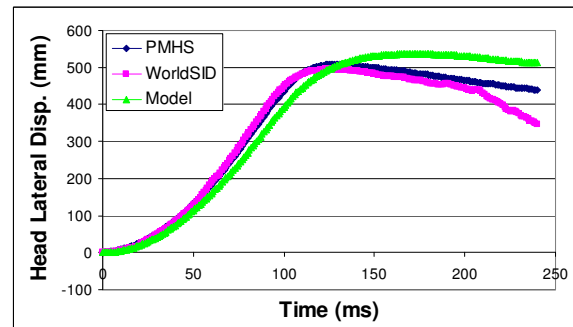


Figure 16. Head lateral displacement – Forward D-ring, 0N Pretension

For the Middle D-ring configuration, the human model predicted a slightly slower velocity to maximum displacement than both the PMHS and WorldSID. The maximum head displacement of the human model was 12% less than the PMHS and 15% less than that of WorldSID. The timing of maximum displacement was within 5ms for all three subjects. All three subjects also predicted rebound of similar velocities subsequent to maximum excursion.

For the Forward D-ring configuration, all the subjects predicted a similar level of maximum displacement (within 5%), and the speed at which they arrive there. When the PMHS reached maximum displacement, the human model's displacement magnitude was within 1% and WorldSID's within 3%.

In contrast to the physical test results, the human model spent in excess of 100ms at 95% of maximum displacement, whereas the PMHS and WorldSID only spent 60ms and 65 ms respectively. This was related to the human model continuing to slip and not rebound in the same way the PMHS and WorldSID did.

DISCUSSION

The aim of this study was to investigate seat belt to shoulder-complex interaction during the first phase of a far-side impact and incorporate this knowledge into a multibody occupant model. After incorporating this into the model, it was to be validated against a series of lateral sled tests using PMHS and WorldSID ATD.

The first aspect of this study involved 1g quasi-static tests using human volunteers, a Hybrid III ATD, a Hybrid III Spring-Spine ATD and the TNO Human Facet Model (with shoulder modifications). From the volunteer quasi-static tests two interesting findings were observed. Firstly, thorax lateral restraint appears to be dependent on seat belt geometry and the level of pretension applied to the belt. Secondly, the critical relationship between the shoulder engaging the belt (or slipping) and seat belt geometry and pretension is highly dependent on human anthropometry. Only two volunteers were needed to demonstrate the uniqueness of humans in this sense.

Due to the effect of anthropometry, it should not be necessary to validate ATDs or human models to a specific human for specific belt pretensions and geometries. It is to be expected that there should be similar restraining effects depending on the level of pretension or belt geometry for human surrogates of similar anthropometry. However, these levels are not possible to estimate until a much larger sample set and higher impact speeds are investigated.

For the meantime, it should be demonstrated that the model or ATD has a critical (or almost critical) slip relation depending on seat belt geometry and pretension levels. Specifically, that it can predict the increasing likelihood of shoulder engagement by the seat belt as the D-ring moves rearward and pretension increases.

The 1g quasi-static simulations indicated that the newly adapted human model was able to demonstrate an increasing level of restraint as D-ring moved rearward and pretension increased. The ATDs tested also predicted this trend, however they were much more sensitive to seat belt geometry changes and pretension. Further to that, the way in which the ATDs loaded the belt was not the same as the volunteer, or the human model for that matter. Restraint in the ATD tests was provided through the belt loading the thorax, whereas the volunteer and human model also loaded the shoulder-complex.

The dimensions of the shoulder ellipsoid added to the human model were derived from the arm radius at the axilla for of a 50th percentile male defined in Tilley et al., (2002). Tilley et al., showed that this 53mm radius coincides with a shoulder breadth of 465mm, very similar to that of this human model. When compared to other anthropometries, a 95th percentile male with a shoulder breadth of 523mm has a radius of 58mm (Tilley et al., 2002). Thus it is reasonable to suggest that the dimensions of the shoulder ellipsoid defined in this study are similar to those of Volunteer 1. Volunteer 2 on the other hand, who had a shoulder breadth of 560mm, is likely to have a larger arm radius at the axilla.

These simulations also indicated that the most critical factor influencing thorax lateral displacement was whether belt slip occurred or not. If the shoulder engaged the belt, displacement levels remained the same regardless of belt geometry or pretension. Similarly, if the belt slipped off the shoulder, there was little influence of belt geometry and pretension.

It was firstly thought that the minor differences observed in overall lateral displacement for cases of belt slip and engagement may be have been a factor of the low test speed (1g). This being related to the fact that occupant models are typically validated at much higher speeds than 1g.

In the high speed sled tests, it was also observed that lateral excursion was only slightly less during shoulder engagement compared to when the belt slipped off the shoulder. The small differences noted in these tests are likely to be influenced by the difference in anthropometry between subjects. Specifically, the PMHS which slipped out of the belt was 13cm shorter than the subject which engaged the belt at the shoulder. While all three subjects distinguished differences in magnitude between the two configurations, the human model showed the largest difference.

The other notable difference between the subjects in the high speed tests related to the shoulder belt loading. This was most pronounced in the case where the belt slipped over the shoulder. The force-time trace for the human model showed two obvious peaks, one related to thorax loading and the other due to arm contact. The same event did not happen in the physical tests. Results from more tests where the belt slips over the shoulder would need to be conducted to see whether this is an artifact of the model or not.

In light of the results put forward in this study, it possible to suggest most likely and least likely configurations for occupants to slip out of the shoulder portion of the seat belt. The most likely configuration being with a forward mounted D-ring, no pretension and slim anthropometry. Conversely, a rear mounted D-ring, pretension and a more solidly built person is less likely to slip out of the shoulder portion of the seatbelt.

Another factor, not investigated in this study, likely to influence belt slip and lateral excursion is occupant height. A taller person is likely to have larger lateral displacement purely based on the belt loading the thorax lower on the inboard side, the increased inertia of the longer body segments and the extra distance their body will occupy when positioned horizontally. As seat belt geometry and occupant size are closely related, further research should be undertaken to gain a better understanding of the effect D-ring position has on lateral excursion.

FUTURE WORK

The next step in this research is for more detailed validation demonstrating that this model is capable of mimicking additional human responses such as neck, thoracic, abdominal and pelvic loading in far-side impacts. This should also be conducted at 60 degrees, as these impacts represent the greatest source of Harm in far-side crashes (Gabler et al., 2005a). The effect of D-ring position and pretension at various impact directions is also to be investigated. Additionally, this model should be validated against tests like those seen in Pintar et al., (2006) to evaluate whether it is capable of identifying which body regions are suitable to load, should inboard countermeasures be proposed.

CONCLUSIONS

The newly adapted human model has been demonstrated to exhibit a critical element of what is required for a far-side occupant model. Specifically, the ability to model seat belt to shoulder-complex interaction. This ability was firstly established using low speed data from volunteer tests and subsequently validated against high speed data obtained from PMHS and WorldSID tests.

This study has also demonstrated that a trend exists between seat belt geometry and pretension on the level of restraint provided to occupants in far-side impacts. It has also been highlighted that human anthropometry has a major effect on the restraint provided by the seat belt in far-side impacts.

ACKNOWLEDGMENTS

The funding for this study is provided in part by the Australian Research Council with cost sharing and support from the other participants. Additional funding for this research has been provided by private parties, who have selected Dr. Kennerly Digges (and the FHWA/NHTSA National Crash Analysis Center at the George Washington University) to be an independent solicitor of and funder for research in motor vehicle safety, and to be one of the peer reviewers for the research projects and reports. Neither of the private parties have determined the allocation of funds or had any influence on the content.

REFERENCES

- Adomeit D, Goegler H, Vu Han V. (1977) "Expected Belt-Specific Injury Patterns Dependent on the Angle of Impact". 3rd International Conference on Impact Trauma, International Research Council on Biokinetics of Impacts, Bron, France, pp. 242-250.
- Boström O, Haland Y. (2003) "Benefits of a 3+2 Point Belt System and an Inboard Torso Side Support in Frontal, Far-Side, and Rollover Crashes". Proceedings of the 18th International Conference on Enhanced Safety of Vehicles, Nagoya, Japan.
- Boström O, Haland Y, Soderstrom P. (2005) "Seat Integrated 3-Point Belt with Reversed Geometry and an Inboard Torso Side-Support Airbag for Improved Protection in Rollover". Proceedings of the 19th International Conference on Enhanced Safety of Vehicles, Washington, DC, USA.
- Chipman M. (2004) "Side Impact Crashes - Factors Affecting Incidence and Severity: Review of the Literature". Traffic Injury Prevention, 5:67-75.
- Digges K, Gabler H, Mohan P, Alonso B. (2005) "Characteristics of the Injury Environment in Far-Side Crashes". Proceedings of the 49th Annual Conference, Association for the Advancement of Automotive Medicine. pp 185 - 197
- Fildes B, Lane J, Lenard J, Vulcan A. (1991) "Passenger Cars and Occupant Injury". Federal Office of Road Safety, Report CR95
- Fildes B, Sparke L, Boström O, Pintar F, Yoganandan N, Morris A. (2002) "Suitability of Current Side Impact Test Dummies in Far-Side Impacts". Proceedings of the 19th International Conference on the Biomechanics of Impact. pp 43-66

Fildes B, Linder A, Douglas C, Digges K, Morgan R, Pintar F, Yoganandan N, Gabler H, Duma S, Stitzel J, Boström O, Sparke L, Smith S, Newland C. (2005) "Occupant Protection in Far Side Crashes".

Proceedings of the 19th International Conference on Enhanced Safety of Vehicles, Washington, DC, USA.

Gabler H, Digges K, Fildes B, Sparke L. (2005a) "Side Impact Injury Risk for Belted Far Side Passenger Vehicle Occupants". Society of Automotive Engineers, Paper 2005-01-0287.

Gabler H, Fitzharris M, Scully J, Fildes B, Digges K, Sparke L. (2005b) "Far Side Impact Injury Risk for Belted Occupants in Australia and the United States". Proceedings of the 19th International Conference on Enhanced Safety of Vehicles, Washington, DC, USA

Horsch J, Schneider D, Kroell C, and Raasch F, (1979) Response of Belt Restrained Subjects in Simulated Lateral Impact. Proceedings of the 23rd Stapp Car Crash Conference, SAE Technical Paper No. 791005, pp. 69-103.

Horsch JD. (1980) "Occupant Dynamics as a Function of Impact Angle and Belt Restraint". Proceedings of the 24th Stapp Car Crash Conference, SAE Technical Paper No. 801310, pp. 417-438.

Kallieris D, Schmidt G. (1990) "Neck Response and Injury Assessment Using Cadavers and the US-SID for Far-Side Lateral Impacts of Rear Seat Occupants with Inboard-Anchored Shoulder Belts", Proceedings of the 34th Stapp Car Crash Conference, SAE Technical Paper No. 902313, pp. 93-100.

Kent R, Shaw G, Lessley D, Crandall J, Svensson M. (2003) Comparison of Belted Hybrid III, THOR, and Cadaver Thoracic Responses in Oblique Frontal and Full Frontal Sled Tests. Society of Automotive Engineers, Paper 2003-01-0160.

de Lange R., van Rooij L., Mooi H., Wismans J. (2005) "Objective Biofidelity Rating of a Numerical Human Occupant Model in Frontal to Lateral Impact". Proceedings of 49th Stapp Car Crash Conference, SAE Technical Paper No. 2005-22-0020, pp. 457-479

Mackay G, Hill J, Parkin S, Munns J. (1993) "Restrained Occupants on the Nonstruck Side in Lateral Collisions". Accident Analysis and Prevention. Vol. 25, No. 2, pp. 147-152.

Otte D, Suren E, Appel H, Nehmzov J. "Vehicle Parts Causing Injuries to Front-Seat Car Passengers in Lateral Impact". Proceedings of 28th Stapp Car Crash Conference, pp. 13-24.

Pintar F, Yoganandan N, Hines M, Maltese M, McFadden J, Saul R, Eppinger R, Khaewpong N, Kleinberger M. (1997) "Chestband Analysis of Human Tolerance to Side Impact", Proceedings of 41st Stapp Car Conference, pp. 63-74.

Pintar F, Yoganandan N, Stemper B, Boström O, Rouhana S, Smith S, Sparke L, Fildes B, Digges K. (2006) "WorldSID Assessment of Far Side Impact Countermeasures", Proceedings of the 50th Annual Conference, Association For The Advancement Of Automotive Medicine.

Rouhana S, Kankanala S, Prasad P, Rupp J, Jeffrey T, Schneider L. (2006) "Biomechanics of 4-Point Seat Belt Systems in Farside Impacts", Proceedings of the 50th Stapp Car Crash Conference, SAE Technical Paper No. 2006-22-0012, pp. 267-298

Sinson G, Yoganandan N, Pintar F. (2003) "Carotid Artery Trauma in Motor Vehicle Crashes: Investigation of the Local Tensile Loading Mechanism". Proceedings of the 20th International Conference on the Biomechanics of Impact. pp 207-216.

Stolinski R, Grzebieta R, Fildes B, Judd R, Wawrzynczak J, Gray I, Mcgrath P, Case M. (1999) "Response of Far Side Occupants in Car-to-Car Impacts with Standard and Modified Restraint Systems using HIII and US SID", SAE Technical Paper No. 1999-01-1321.

Tilley, A. R and Henry Dreyfuss Associates (2002). "The Measure of Man and Woman: Human Factors Design". Revised Edition. Published by John Wiley and Sons, Inc. United States of America.

Tornvall F, Svensson M, Davidsson J, Flogard A, Kallieris D, Haland Y. (2005) "Frontal Impact Dummy Kinematics in Oblique Frontal Collisions: Evaluation Against Post Mortem Human Subject Test Data". Traffic Injury Prevention, 6:340-350.